Nonlinear Processes in Geophysics (2000) 7: 201–209

Nonlinear Processes in Geophysics

MHD effects of the solar wind flow around planets

H. K. Biernat[1,2], N. V. Erkaev[3], C. J. Farrugia[4], D. F. Vogl[1,2], and W. Schaffenberger[1]

[1]Space Research Institute, Austrian Academy of Sciences, Graz, Austria
[2]also at: Institute for Geophysics, Astrophysics, and Meteorology, University of Graz, Austria
[3]Institute of Computational Modelling, Russian Academy of Sciences, Krasnoyarsk, Russia
[4]Institute for the Study of Earth, Oceans, and Space, University of New Hampshire, Durham, USA

Received: 8 November 1999 – Revised: 18 February 2000 – Accepted: 21 March 2000

Abstract. The study of the interaction of the solar wind with magnetized and unmagnetized planets forms a central topic of space research. Focussing on planetary magnetosheaths, we review some major developments in this field. Magnetosheath structures depend crucially on the orientation of the interplanetary magnetic field, the solar wind Alfvén Mach number, the shape of the obstacle (axisymmetric/non–axisymmetric, etc.), the boundary conditions at the magnetopause (low/high magnetic shear), and the degree of thermal anisotropy of the plasma. We illustrate the cases of Earth, Jupiter and Venus. The terrestrial magnetosphere is axisymmetric and has been probed in situ by many spacecraft. Jupiter's magnetosphere is highly non–axisymmetric. Furthermore, we study magnetohydrodynamic effects in the Venus magnetosheath.

1 Introduction

The study of the interaction of the solar wind with planets forms a central object of space research. On approach to a planetary obstacle, the supersonic and super-Alfvénic, magnetized solar wind flow is thermalized and made subsonic at a bow shock standing off from the obstacle. The shocked solar wind then flows in the magnetosheath past the planet. The plasma and magnetic field behaviour in the magnetosheath is the subject of numerous investigations both theoretically and observationally (e.g., Spreiter and Stahara (1994); Erkaev et al. (1999); Song et al. (1992); Song and Russell (1997)).

Early approaches to the study of the flow in the magnetosheath were essentially based on gasdynamics (Spreiter et al. (1966), Spreiter and Stahara (1994)). Gasdynamics predicted the stand–off distance of the bow shock and plasma and flow parameters downstream of it. Once the flow was thus determined, the magnetic field in the magnetosheath was obtained in a kinematic approximation. This is the gasdynamic convected magnetic field (GDCF) model. Thus in the GDFC model, the plasma parameters result from the pure gas dynamic system of equations, and the magnetic field is then obtained from the equations of magnetic flux conservation and magnetic induction. This widely used approach predicted successfully a number of magnetosheath features. It also reproduced the draping of magnetic field lines around the magnetosphere. The magnetic field calculated in the kinematic approximation has, however, a strong singularity at the magnetopause, requiring for its removal consideration of the effect of the magnetic field on the flow by including the field in the momentum equation. Two ways have been explored in the solution of this problem: (a) semi-analytical and (b) global 3-dimensional simulations. Among the work which addressed this problem semi-analytically were Midgley and Davis (1963), Lees (1964), Zwan and Wolf (1976), Erkaev (1988), Erkaev and Mezentsev (1992).

Zwan and Wolf (1976) presented a model where they showed that the plasma density decreases toward the magnetopause while simultaneously the magnetic field piles up against this boundary. The region close to the magnetopause is called the plasma depletion layer (PDL). In the Zwan and Wolf approach, its sunward edge is defined by a 100% drop of the density with respect to its value immediately downstream of the bow shock. The magnetic field pile–up and density decrease depend not only on the parameters of the interplanetary magnetic field (IMF) and the solar wind, but also on boundary conditions at the magnetopause, generally speaking, whether the magnetopause is a tangential or a rotational discontinuity. Since its introduction, the PDL has formed a cornerstone of investigations of the flow problem, both in theoretical as well as in observational work (e.g., Erkaev (1988), Paschmann et al. (1993), Phan et al. (1994), Anderson et al. (1994),

Correspondence to: H. K. Biernat

Erkaev et al. (1998), Erkaev et al. (1999), Biernat et al. (1995), Farrugia et al., 1995, 1997a, 1998)

In order to compute the 3–dimensional structure of the PDL, Erkaev (1988) and Erkaev and Mezentsev (1992) elaborated a boundary layer approach, i.e., one where the total pressure normal to the layer is constant. This method has been extended to the whole magnetosheath (Erkaev et al. (1998), and references therein). Among the 3-dimensional, global MHD models we mention those of Wu (1992) and Cairns and Lyon (1995). In Wu's model, the large–scale features of the MHD flow around Earth, and position of the shock are reproduced well. However, the PDL (or magnetic barrier) is not reproduced properly in this simulation: The plasma density has only a small decrease ahead of the magnetopause. Cairns and Lyon (1995) studied the stand-off distance of the bow shock as a function of solar wind Alfvén Mach number and pointed out clear discrepancies between MHD predictions and gasdynamics: The magnetosheath predicted by the MHD model is thicker than that in pure gasdynamics, an effect also seen at Venus (Zhang et al. (1990), Biernat et al. (1999)). The effect is more pronounced for low Alfvén Mach numbers, and depends also sensitively on the angle that the IMF subtends with the velocity (cone angle). The structure of the flow in the magnetosheath was beyond the scope of the work of Cairns and Lyon (1995).

In this paper we discuss the following topics: (a) the terrestrial magnetosheath structure for low magnetic shear at the magnetopause in its dependence on the Alfvén Mach number, (b) the anisotropy of the plasma, (c) magnetosheath effects for planets with non–axisymmetric magnetospheres, and (d) aspects of MHD flow about Venus.

2 The terrestrial magnetosheath

Supersonic solar wind flow interacting with Earth produces a detached shock wave which separates the unperturbed solar wind from the magnetosheath. The changes in field and flow parameters are given by the Rankine-Hugoniot relations (e.g., Petrinec and Russell (1997)):

$$\left[\!\left[\rho u_n^2 + \Pi\right]\!\right] = 0, \quad \left[\!\left[\rho u_n \mathbf{u}_\tau - \frac{B_n}{4\pi}\mathbf{B}_\tau\right]\!\right] = 0, \tag{1}$$

$$\left[\!\left[\rho u_n\right]\!\right] = 0, \quad \left[\!\left[B_n\right]\!\right] = 0, \quad \left[\!\left[(\mathbf{u}\times\mathbf{B})_\tau\right]\!\right] = 0, \tag{2}$$

$$\left[\!\left[\rho u_n\left[\frac{u^2}{2} + \left(\frac{\gamma}{\gamma-1}\right)\frac{p}{\rho}\right] + \frac{u_n B^2 - B_n(\mathbf{u}\cdot\mathbf{B})}{4\pi}\right]\!\right] = 0. \tag{3}$$

Here, ρ, $\mathbf{u}$, and $\mathbf{B}$ are the mass density, velocity and magnetic field, respectively. Π is a total pressure, i.e., $\Pi = p + B^2/(8\pi)$ and γ is the adiabatic parameter. The symbol $[X]$ stands for the difference in quantity X across the shock. Subscripts n and τ represent quantities normal and tangential to the shock surface, respectively. At the magnetopause modelled as a tangential discontinuity we have the no-flow condition: $u_n = 0$.

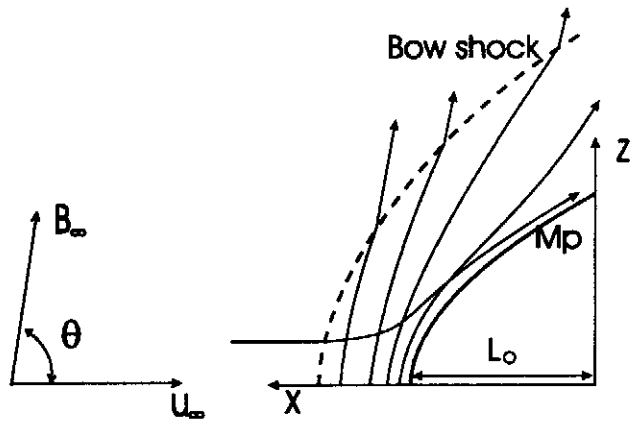

Fig. 1. Geometric situation of the problem.

For the magnetosheath plasma considered to be a perfectly conducting inviscid gas we have the system of MHD equations without dissipation:

$$\rho\frac{\partial \mathbf{u}}{\partial t} + \rho(\mathbf{u}\cdot\nabla)\mathbf{u} + \nabla\Pi - \frac{1}{4\pi}(\mathbf{B}\cdot\nabla)\mathbf{B} = 0 \tag{4}$$

$$\frac{\partial \mathbf{B}}{\partial t} - \nabla\times(\mathbf{u}\times\mathbf{B}) = 0, \quad \nabla\cdot\mathbf{B} = 0, \tag{5}$$

$$\frac{\partial \rho}{\partial t} + \nabla\cdot(\rho\mathbf{u}) = 0, \quad \frac{\partial}{\partial t}\left(\frac{p}{\rho^\gamma}\right) + (\mathbf{u}\cdot\nabla)\left(\frac{p}{\rho^\gamma}\right) = 0. \tag{6}$$

The problem is to find a solution of the MHD system (4–6) with given parameters of the unperturbed flow and with the boundary conditions on the shock wave and on the obstacle surface. In contrast to gasdynamic models, we include *ab initio* the magnetic field in the momentum equation, which is of particular need in the PDL. The flow in this region is dominated by the magnetic field. The geometry of the problem is shown in Fig. 1.

The main assumption we use in integration of equations (4–6) is that the total pressure is a prescribed function of the coordinates. As a first approximation, we use the so-called Newtonian formula (Petrinec and Russell (1997)) for the total pressure along the magnetopause, $\Pi_m = (\Pi_0 - \Pi_\infty)\cos^2\psi + \Pi_\infty$, where Π_0 is the pressure at the subsolar point of the magnetopause, Π_∞ is the pressure in the upstream medium, and ψ denotes the angle between the stagnation stream line and the normal to the magnetopause. The variation of the total pressure between the magnetopause and the bow shock is approximated as a quadratic function of the distance to the magnetopause, μ, $\Pi = \Pi_m(1-\mu^2/\Delta^2) + \Pi_S\mu^2/\Delta^2$, where Π_m and Π_S are the values at the magnetopause and immediately downstream of the bow shock, respectively, and Δ is the thickness of the magnetosheath. This quadratic dependence is chosen because it agrees best with observations (Farrugia et al. (1997b)).

The shock front is taken to be a spherically symmetric hyperboloid parameterized by three quantities a, L_S,

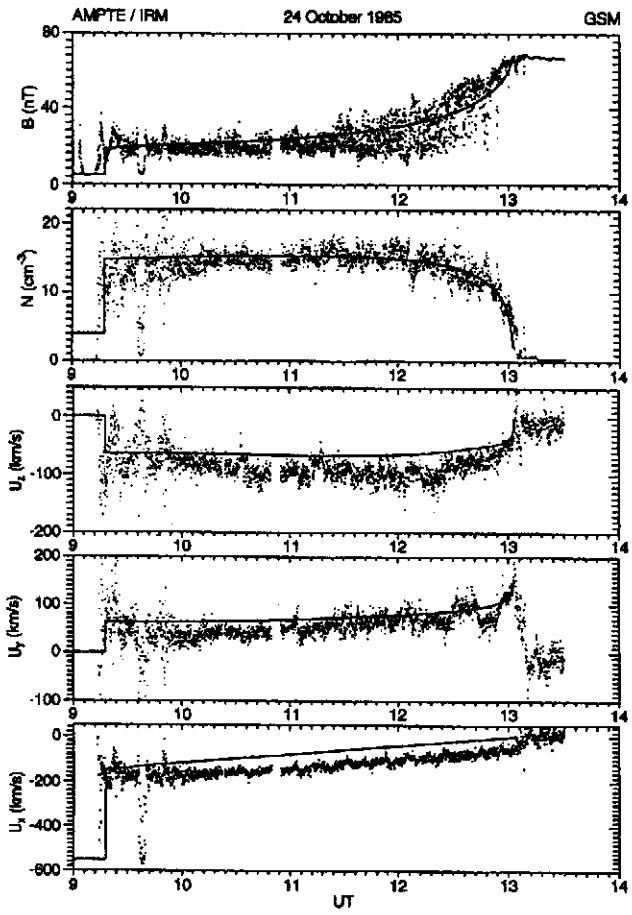

Fig. 2. Computed profiles compared with AMPTE/IRM spacecraft data.

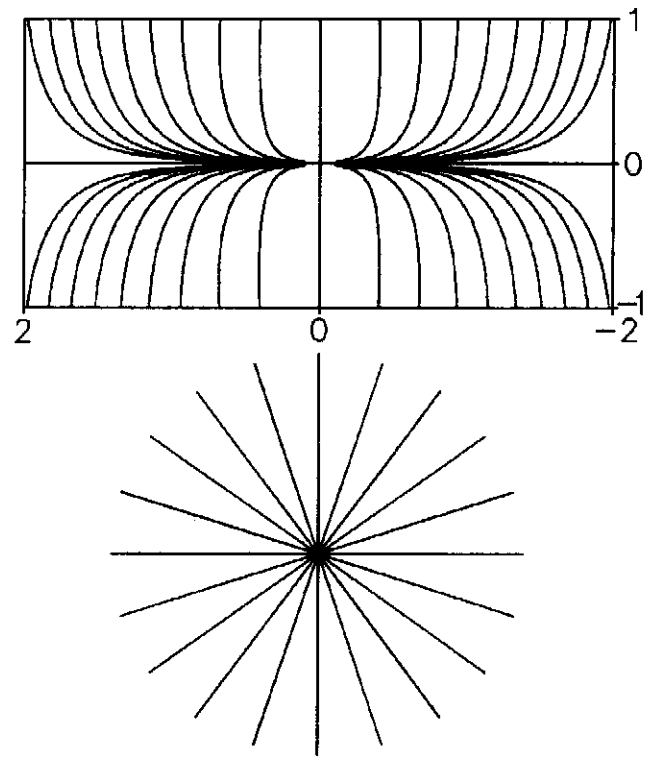

Fig. 3. Stream lines at the magnetopause as seen from the Sun. Top: Plasma stream lines in an MHD approach. Bottom: Stream lines modelled in gasdynamics.

and d, $X = L_S\{-a[1 + Z^2/(aL_S^2) + Y^2/(aL_S^2)]^{1/2} + a\} + d + L_0$, where L_S is a radius of curvature of the shock front at the subsolar point, a is the cotangent squared of the polar angle of the Mach cone at infinity, d is the thickness of the subsolar magnetosheath, and L_0 is the radius of curvature of the subsolar magnetopause. With the assumptions formulated above, we obtain a numerical solution of the flow problem by using a finite difference Lax-Wendroff scheme and frozen-in material coordinates (see, e.g., Biernat et al. (1995)).

In Fig. 2 we show the computed profiles of magnetic field, density, and components of velocity, which are compared with spacecraft data (after Farrugia et al. (1998)). The observations were made during an inbound crossing of the near-subsolar magnetosheath by the AMPTE/IRM spacecraft. The chosen interval contains a solar wind part, the bow shock crossing, the magnetosheath, and parts of the outer magnetosphere. In the theoretical description, the bow shock is modelled as a fast shock. During the crossing of the magnetopause at $\sim$ 1300 UT, the magnetic shear is low (15°), so that we do not expect magnetic reconnection to occur. As noted in Farrugia et al. (1998), the data on this pass do not show evidence of a slow shock. The data of the crossing are shown as points, and the model predictions as solid lines. The spacecraft first encounters non-steady conditions, evidenced by two bow shock crossings between 0900 and 0940 UT. Thereafter, the inbound magnetosheath crossing is under steady conditions (Phan et al., 1994). The model reproduces the variation of all parameters very well. The behaviour of the magnetic field and density is typical of a magnetic barrier or a plasma depletion layer next to the low-shear magnetopause, occupying in this case 20 min of a 3.8 hour pass. The non-axisymmetric flow pattern is clear: while the field-aligned velocity component, U_z decreases to 0, the component perpendicular to the field, U_y, increases. The acceleration of the plasma in the y direction is due to magnetic tension.

Qualitatively, the formation of the plasma depletion layer can be understood from the frozen-in condition, $B/\rho \sim l$, where l is the distance between fluid elements on the same field line. On approach to the magnetopause, where the flow is diverted past the obstacle, l increases, so that B increases and ρ decreases.

The flow pattern obtained from our MHD solution is of stagnation line type, in contrast to the stagnation point flow expected from gasdynamics. This result supports the hypothesis of Sonnerup (1974), who first pro-

posed the idea of a stagnation line flow structure near the magnetopause. In Figure 3 we demonstrate the influence of the magnetic field on the plasma flow in the vicinity of the magnetopause. The figure shows stream lines as seen from the Sun modelled by magnetohydrodynamics (top) and gasdynamics (bottom). In the first case, the stream lines are not radial, and each stream line touches the stagnation line, directed along the horizontal IMF. In the second case, because of the vanishing magnetic field, the stream lines radiate away from the subsolar point as straight lines.

We mention that there is considerable interest in a phenomenon called slow mode transition. This terminology was introduced to describe a local density peak sometimes observed in the magnetosheath density profile with magnetic pressure varying in antiphase with the plasma pressure. This occurs just before the density decreases in the depletion layer (Song et al. (1992)). A theoretical explanation of this phenomenon was proposed by Southwood and Kivelson (1995) who suggested the presence of an MHD slow shock wave standing inside the magnetosheath just ahead of the magnetopause. Our steady–state MHD solution with a no–flow condition at the magnetopause does not have this structure (see Erkaev et al. (1998)). It may be that it is related to nonsteady conditions or reconnection effects at the magnetopause, which we have not discussed here.

3 Thermal anisotropy of the magnetosheath plasma

So far we have considered the plasma to have isotropic pressure. However, many studies of the terrestrial magnetosheath indicate that the plasma is anisotropic with $T_\perp > T_\parallel$ (e.g. Gary et al., 1994).

To study magnetosheath structure in a case of anisotropy, one has to apply the anisotropic MHD system of equations as follows:

$$\rho(\mathbf{u}\cdot\nabla)\mathbf{u} + \nabla\cdot\mathbf{P} + \frac{1}{8\pi}\nabla B^2 - \frac{1}{4\pi}(\mathbf{B}\cdot\nabla)\mathbf{B} = 0, \qquad (7)$$

$$\nabla\cdot[\rho\mathbf{u}(u^2/2 + \frac{1}{4\pi}B^2/\rho + \mathcal{E}) + \mathbf{P}\cdot\mathbf{u} - \frac{1}{4\pi}(\mathbf{B}\cdot\mathbf{u})\mathbf{B}] = 0, \qquad (8)$$

$$\nabla\cdot(\rho\mathbf{u}) = 0, \quad \nabla\times(\mathbf{u}\times\mathbf{B}) = 0, \quad \nabla\cdot\mathbf{B} = 0. \qquad (9)$$

Here, $\mathbf{P}$ is the pressure tensor $P_{ik} = P_\perp\delta_{ik} + (P_\parallel - P_\perp)B_iB_k/B^2$ introduced by Chew et al. [1956], and $\mathcal{E}$ is the thermal energy, $\mathcal{E} = P_\perp/\rho + 0.5P_\parallel/\rho$.

The problem arises how to close the anisotropic MHD equations. Double adiabatic theory (Chew et al., 1956) has been shown to be inappropriate for the magnetosheath (Hill et al. (1995)). AMPTE/CCE and IRM observational studies (Phan et al. (1994), Anderson et al. (1994)) showed that there is an anticorrelation between

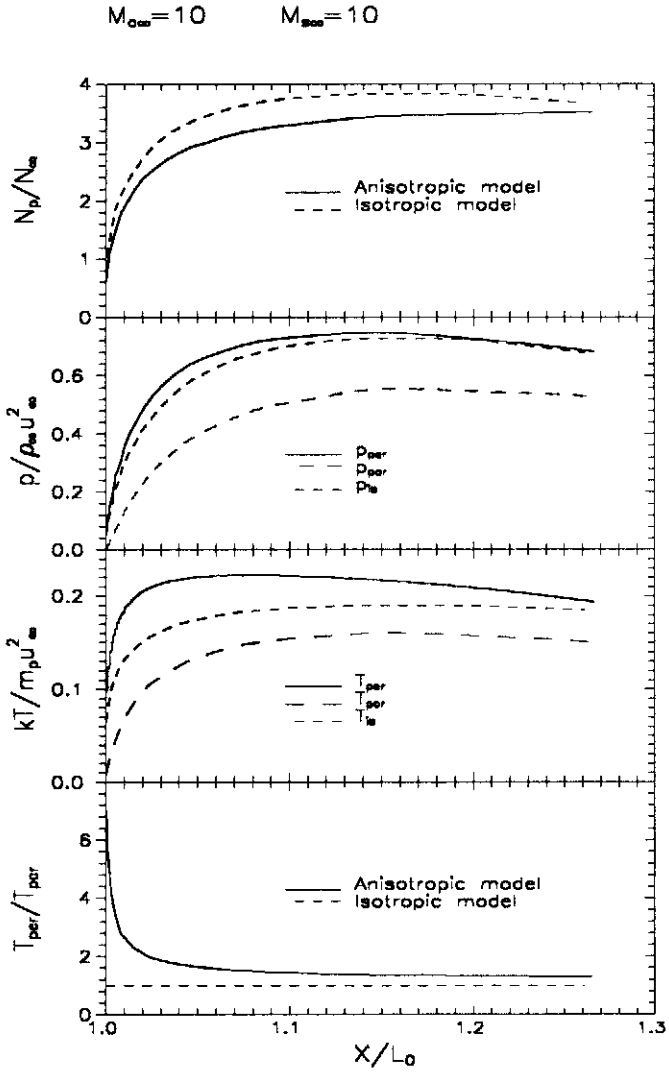

Fig. 4. Anisotropic model compared with the isotropic model.

the temperature anisotropy $A_p = T_\perp/T_\parallel - 1$ and the proton beta parallel to the magnetic field, $A_p = 0.85\beta_\parallel^{-0.5}$. This relation has later been suggested as a suitable closure relation for the ideal MHD equations, and is used in the "Bounded Anisotropy Model" (Denton et al., 1994). We use this anticorrelation to close the system of equations. A first discussion of the evolution of $T_\perp/T_\parallel$ in the magnetosheath was made in a 2-D simulation (Denton and Lyon, 1996), where it is shown that the depletion effect is enhanced by anisotropy.

An extension of the model in section 2 to include anisotropies through the Bounded Anisotropy Model Ansatz was put forward by Erkaev et al. (1999). Results of this model are shown in Fig. 4 where they are contrasted with results assuming isotropy. The panels show from top to bottom the density, the plasma pressures, the temperature, and the ratio $T_\perp/T_\parallel$. The Alfvén Mach number and the sonic Mach number are equal 10. The quantities are normalized as shown in Fig. 4. The re-

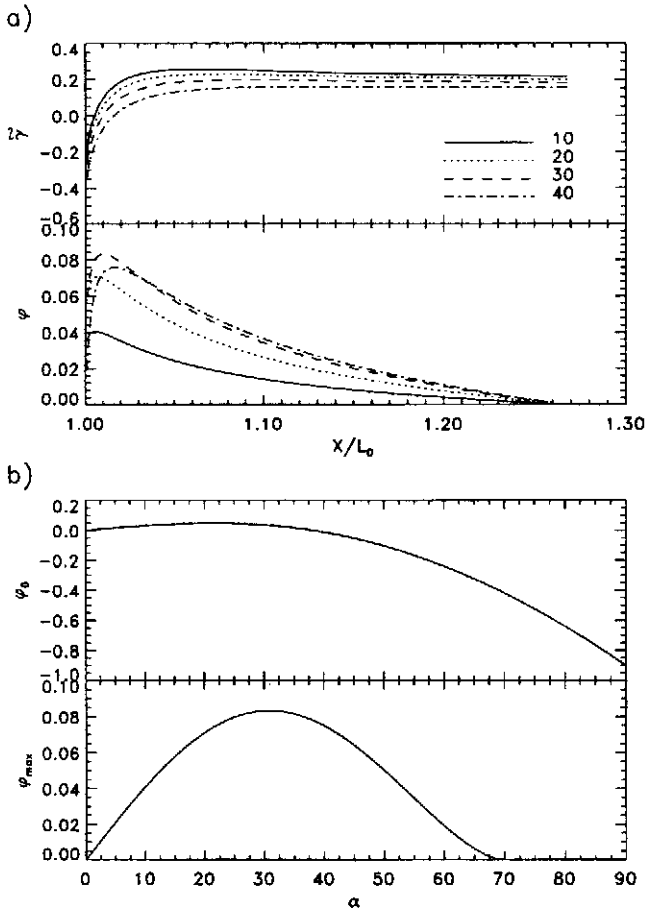

Fig. 5. Characteristics of the mirror instability between the bow shock and the magnetopause.

sults of the isotropic model are shown by short dash lines. In the anisotropic model, the density, the parallel and perpendicular temperatures, and plasma pressures all decrease toward the magnetopause. Profiles of quantities parallel to the magnetic field lie below those of the corresponding quantities perpendicular to the field, with isotropic variations lying between these two extremes. Anisotropy has a considerable effect on the density profile, which lies below that in the isotropic limit throughout the magnetosheath.

A theoretical result supported by data is that the main body of the magnetosheath is marginally mirror unstable, and the region next to the magnetopause is unstable to electromagnetic ion cyclotron waves. Mirror mode waves may be seen in the data in Fig. 2, with their strongly compressive nature.

The characteristics of the mirror instability between the magnetopause and the bow shock are shown in Fig. 5 between the bow shock and the magnetopause. The first panel in (a) shows the growth rate ($\tilde{\gamma}$) of the mirror instability as a function of distance along the subsolar line. This growth rate is normalized to $k_{\|} V_t$, where $k_{\|}$ is the component of the wave number along the magnetic field and V_t is the thermal velocity of protons. All curves are parameterized by angles α between the wave vector and subsolar line.

The second panel in (a) shows the function $\varphi(x)$ which is defined as the integral: $\varphi = \int_{x_s}^{x} (\tilde{\gamma} v_p / v_x) \sin\alpha dx$. This function determines the growth in amplitude of the mirror fluctuations from the bow shock to the magnetopause $\delta B = \delta B_0 \exp(k L_0 \varphi(x))$, where L_0 is a curvature radius of the subsolar magnetopause.

In the two panels of Fig. 5b, the first quantity, φ_0, is the value of the function $\varphi(x)$ at the subsolar point, $\varphi_0 = \varphi(1)$, and the second quantity, φ_{max} is the maximum of the function $\varphi(x)$. Both quantities are shown as functions of the angle between wave vector and the subsolar line.

One can see from the plot that the largest value of maximum of the function $\varphi(x)$ (~ 0.08) corresponding to $\alpha = 30°$ occurs very near to the magnetopause. Mirror fluctuations are expected to have their largest amplitude here. Analyzing parameter φ_0, we conclude that the mirror fluctuations are very small at the magnetopause for a whole range of α. These predictions of the intensity of the mirror fluctuations are in qualitative agreement with the panel of magnetic fluctuations shown in Fig. 2. However, a quantitative prediction of the magnetic fluctuations requires a nonlinear analysis of the mirror instability.

4 Magnetosheaths of non-axisymmetric magnetospheres

Jupiter has a planetary magnetosphere which departs strongly from axisymmetry, its radius of curvature in the equatorial plane being much larger than that orthogonal to this plane. We thus model the Jovian magnetosphere by a paraboloid with two radii of curvature. With respect to axisymmetric magnetospheres, the magnetosheaths of non-axisymmetric magnetospheres have two properties. It is found that the thickness of magnetosheath and PDL depend sensitively on the orientation of the IMF, decreasing monotonically as the inclination of the IMF to the rotational equator (the plane perpendicular to the rotation axis) decreases. For an arbitrary orientation of the IMF, the magnetosheath magnetic field along the stagnation streamline is not only compressed as the magnetopause is approached; it also rotates smoothly toward the Jovian rotation axis.

Model calculation of these effects are shown in Fig. 6. Figure 6a plots profiles of magnetosheath magnetic field and density for 7 different orientations of the IMF, where 90° signifies an IMF directed in the rotational equator. The pile-up of the field is evident in all profiles. However, as the IMF rotates towards the equator this field pile-up becomes stronger and is confined more and more to the region next to the magnetopause. This is a clear sign that the PDL is weaker as this angle increases. Cor-

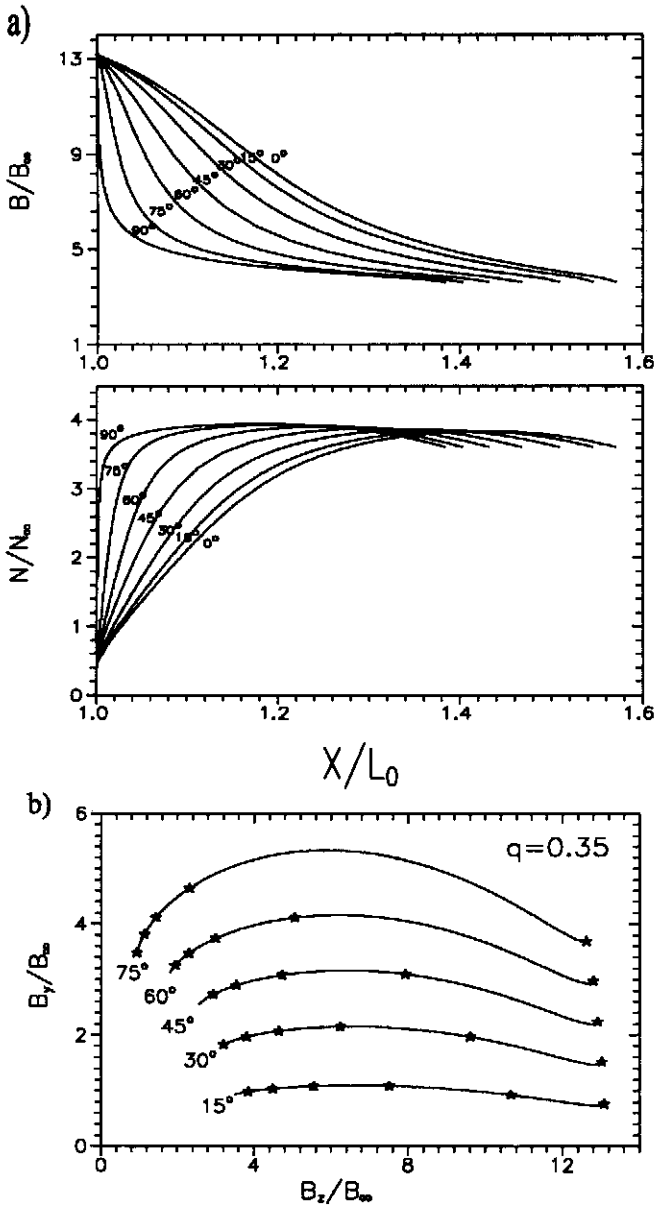

Fig. 6. Effects of a non-axisymmetric magnetosphere.

respondingly, the magnetosheath thickness also shrinks. Figure 6b shows hodographs of the magnetic field for different values of this angle. Each plot extends from the bow shock (left) to the magnetopause, showing an increase and rotation of the field. On each curve, the interval between star symbols represent equal intervals along the Sun-Jupiter axis.

5 The magnetosheath of Venus

In this section we focus on some aspects of MHD flow past Venus and on the stand–off distance of the bow shock of Venus. Venus is an unmagnetized planet. For unmagnetized planets, the solar wind is stood off by the ionospheric pressure at the ionopause, which plays

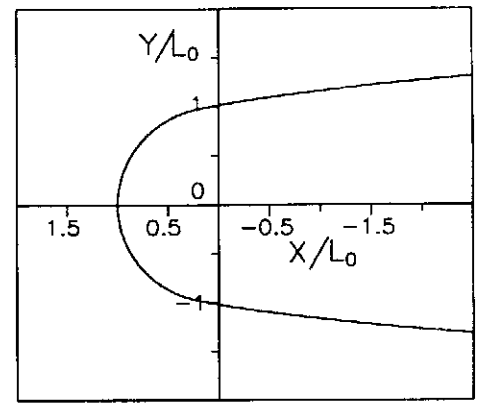

Fig. 7. Projection on the ecliptic (XY) plane of the model shape of Venus. The surface of a hemisphere on the sunward side is smoothly matched to that of a truncated cone on the nightside.

the role of the magnetopause at magnetized planets. There is a considerable discrepancy between the magnetosheath thickness as modelled by GDCF and in situ observations, the gasdynamic model magnetosheath being thinner. Zhang et al. (1993) found that if one includes mass loading resulting from exospheric pick–up processes, the bow shock stand–off distance does not significantly increase. Thus, we formulate an MHD model for the magnetosheath of Venus to reduce the discrepancy between theory and observation.

We model the ionopause by a composite surface made up of the surface of a hemisphere (of radius L_0) on the sunward side smoothly attached to the surface of a truncated cone (see Fig. 7). With X oriented from Venus towards the Sun, we have (in quantities normalized to L_0),

$$X = \begin{cases} 1.4 - 1.3r^4, & r \geq 0.98, \\ \sqrt{1-r^2}, & r \leq 0.98, \end{cases} \tag{10}$$

where $r^2 = \sqrt{Y^2 + Z^2}$.

hspace*0.35cm Fig. 8 shows the results of the MHD calculations. From top to bottom we show the magnetic field strength, number density, temperature, and speed flow respectively. The ionopause is on the left at $X/L_0 = 1$, and the curves are continued until the jump at the bow shock. The direction of the IMF is assumed to be perpendicular to the solar wind velocity. Results are shown for six different free–stream Alfvén Mach numbers, $M_{A\infty} = 5, 8, 10, 15, 20, 25$, and the sonic Mach number, $M_{S\infty} = 10$. This chosen parameter range covers typical values near Venus (e.g. Luhmann et al., 1993). For example, for $M_{A\infty} = 5$ and $M_{S\infty} = 10$, we obtain a magnetosonic Mach number of 4.5, the same as reported in Zhang et al. (1993).

We next study the standoff distance of the bow shock. From Zhang et al. (1990) we conclude that for a magnetosonic Mach number of 4.5 and a specific heat ratio of 5/3, the GDCF model yields the following discrepancy.

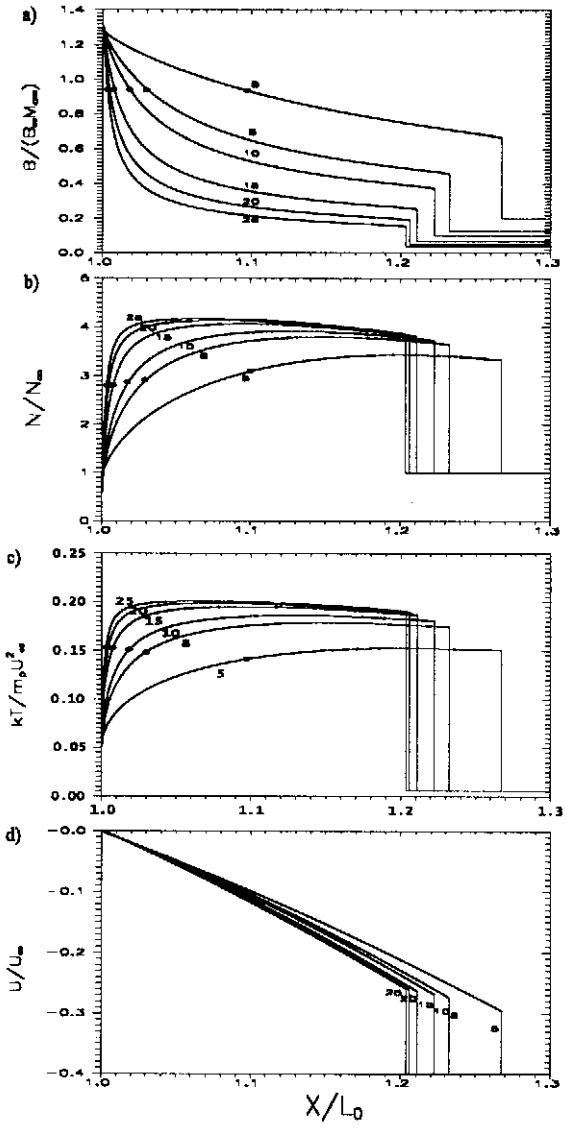

Fig. 8. Profiles of the (a) magnetic field B, (b) density N, (c) temperature T, and (d) bulk velocity U for six representative values of the solar wind Alfvén Mach number, $M_{A\infty} = 5, 8, 10, 15, 20, 25$. The sonic Mach number is $M_{S\infty} = 10$.

If the scale height is chosen to match the ionopause location ($H/L_0 = 0.03$, where L_0 is the obstacle radius at the nose), the computed bow shock is too close to the planet, namely, at $\sim 0.24 L_0$, whereas the observed position is at $\sim 0.28 L_0$. This yields a relative percentage discrepancy between data and gasdynamic modeling of $(0.28 - 0.24) \times L_0/(0.28 \times L_0)$. That is, with respect to observations, the magnetosheath is narrower in the Venus–Sun direction by $\sim 14\%$.

We study the case of $M_{A\infty} = 5$ and $M_{S\infty} = 10$. From this we get the magnetosonic Mach number $M_{ms} = M_{A\infty} M_{S\infty}/(M_{S\infty}^2 + M_{A\infty}^2)^{1/2} = 4.5$, the value reported by Zhang et al. (1990). The top curve of the first panel of Fig. 8 shows the magnetic field behaviour for this case. It is seen that the subsolar bow shock is located $\sim 0.27\ L_0$ from the ionopause. Our MHD model thus yields a discrepancy with observations of $(0.28 - 0.27) \times L_0/(0.28 \times L_0) \sim 3.6\ \%$, which is a substantial improvement over gas dynamics.

6 Conclusions

Planetary magnetosheath structure is strongly dependent on the IMF and the shape of the magnetosphere. For high Alfvén Mach number, the most crucial parameter is the IMF component orthogonal to the solar wind velocity. One effect is that this component causes an essential enhancement of the magnetosheath thickness. Another important effect is that this component is directly related with the PDL, where the magnetic field eventually exerts a strong influence on the flow. The thickness of the PDL is proportional to the inverse square of the Alfvén Mach number defined for the IMF component transverse to the solar wind velocity (Farrugia et al. (1995), Farrugia et al. (2000)).

In our MHD model we have shown the different behaviour of field-aligned and perpendicular components of velocity along a given normal to the obstacle. While the parallel velocity decreases towards the magnetopause the perpendicular velocity increases. The results of calculation show that the density, temperature, and plasma pressure decrease along a normal to the obstacle. Stream lines tend to be orthogonal to magnetic field lines near magnetopause. At the low shear magnetopause, stream lines have a specific structure with a stagnation line oriented parallel to the IMF. Contours of plasma parameters are not axisymmetric lines near the magnetopause. All parameters have a minimal gradient in the direction of the IMF. The gradients of all parameters along the normal to the obstacles increase with increasing Alfvén Mach number.

In the case of temperature anisotropy the ratio of perpendicular and parallel temperatures is bounded by the mirror or ion cyclotron instabilities. The variations of the plasma beta, pressure, and temperature across the subsolar magnetosheath in the isotropic limit lie between variations of the corresponding quantities perpendicular (as an upper bound) and parallel to the field. In the anisotropic model the density is smaller than that in the isotropic limit throughout the magnetosheath.

There are two main effects caused by a non-axisymmetric shape of the magnetosphere. Firstly, there is a strong dependence of the magnetosheath thickness and plasma depletion effect on the clock angle of the IMF. The second effect is the rotation of the magnetosheath field direction toward the plane of lesser curvature. These effects are absent in a case of axisymmetry.

Furthermore we have presented numerical MHD calculations for flow around Venus. We computed results for a wide range of Alfvén Mach numbers, $M_{A\infty} = 5, 8, 10, 15, 20, 25$, encompassing typical interplanetary

values of this parameter at Venus's orbit and for the typical value of the sonic Mach number, $M_{S\infty} = 10$. The influence of decreasing Alfvén Mach number (i.e., increasing influence of the IMF) is reflected in wider magnetosheaths, wider plasma depletion layers, gradients in parameter variations extending throughout the entire magnetosheath (rather than being concentrated near the ionopause), and weaker magnetic field pileup at the ionopause. The increase of B and the simultaneous decrease of N occurring near the ionopause constitute a magnetic barrier at Venus. This feature is seen in the terrestrial magnetosheath near the low-shear magnetopause (plasma depletion layer) (e.g. Phan et al., 1994). We showed that the discrepancy between gasdynamics and observations can be substantially diminished, and that the Alfvén Mach number has a strong influence on the Venus magnetosheath.

Acknowledgements. Part of this work was done while NVE and CJF were on a research visit to the Space Research Institute of the Austrian Academy of Sciences in Graz. This work is supported by the Austrian "Fonds zur Förderung der wissenschaftlichen Forschung" under project P12761-TPH, by grant No 98-05-65290 from the Russian Foundation of Basic Research, by grant No 97-0-13.0-71 from the Russian Ministry of Education, and by NASA grant NAG5-2834.

References

Anderson, B. J., Fuselier, S. A., Gary, S. P., and Denton, R. E., Magnetic spectral signatures in the Earth's magnetosheath and plasma depletion layer, *J. Geophys. Res.*, *99*, 5877-5891, 1994.

Biernat, H. K., Bachmaier, G. A., Kiendl, M. T., Erkaev, N. V., Mezentsev, A. V., Farrugia, C. J., Semenov, V. S., and Rijnbeek, R. P., Magnetosheath parameters and reconnection: A case study for the near-cusp region and the equatorial flank, *Planet. Space Sci.*, *43*, 1105, 1995.

Biernat, H. K., Erkaev, N. V., and Farrugia, C. J., Aspects of MHD flow about Venus, *J. Geophys. Res.*, *104*, 12617-12626, 1999.

Cairns, I. H. and Lyon, J. V., MHD simulation of the Earth's bow shock at low Mach numbers: Stand-off distances, *J. Geophys. Res.*, *100*, 17173, 1995.

Chew, G. F., Goldberger, M. L., and Low, F. E., The Boltzmann equation and the one-fluid hydromagnetic equations in the absence of particle collisions, *Proc. R. Soc., London*, Ser. A., *236*, 112, 1956.

Denton, R. E., Anderson, B. J., Gary, S. P., and Fuselier, S. A., Bounded anisotropy fluid model for ion temperatures, *J. Geophys. Res.*, *99*, 11225, 1994.

Denton, R. E. and Lyon, J. G., Density depletion in an anisotropic magnetosheath, *Geophys. Res. Lett.*, *23*, 2891, 1996.

Erkaev, N. V., Results of the investigation of MHD flow around the magnetosphere, *Geomagn. Aeron.*, *28*, 529, 1988.

Erkaev, N. V. and Mezentsev, A. V., The flow of the solar wind around the magnetosphere and the generation of electric field, *Solar Wind-Magnetosphere Interaction*, ed. by M. F. Heyn et al., Vienna, Austria, 43-66, 1992.

Erkaev, N. V., Farrugia, C. J., and Biernat, H. K., Comparison of Gasdynamic and MHD predictions for Magnetosheath Flow, in *Polar Cap Boundary Phenomena*, ed. by J. Moen et al., Kluwer Academic Publishers, 27-40, 1998.

Erkaev, N. V., Farrugia, C. J., and Biernat, H. K., Three-dimensional, one-fluid, ideal MHD model of magnetosheath flow with anisotropic pressure, *J. Geophys. Res.*, *104*, 6877-6887, 1999.

Farrugia, C. J., Erkaev, N. V., Biernat, H. K., and Burlaga, L. F., Anomalous magnetosheath properties during Earth passage of an interplanetary magnetic cloud, *J. Geophys. Res.*, *100*, 19245-19257, 1995.

Farrugia, C. J., Erkaev, N. V., Biernat, H. K., Lawrence, G. R., and Elphic, R. C., Plasma depletion layer model for low Alfvén Mach number: Comparison with ISEE observations, *J. Geophys. Res.*, *102*, 7087-7093, 1997a.

Farrugia, C. J., Erkaev, N. V., Biernat, H. K., and Burlaga, L. F., Dependence of magnetosheath properties on solar wind Alfvén Mach number and magnetic shear across the magnetopause, *The Solar Wind-Magnetosphere System 2*, ed. by H. K. Biernat et al., Vienna, Austria, 95-108, 1997b.

Farrugia, C. J., Biernat, H. K., Erkaev, N. V., Kistler, L. M., Le, G., and Russell, C. T., MHD model of magnetosheath flow: Comparison with AMPTE/IRM observations on 24 October, 1995, *Ann. Geophys.*, *16*, 518-527, 1998.

Farrugia, C. J., Erkaev, N. V., Biernat, H. K., On the effects of solar wind dynamic pressure on the anisotropic terrestrial magnetosheath, *J. Geophys. Res.*, *105*, 115, 2000.

Gary, S. P., Anderson, B. J., Denton, R. E., Fuselier, S. A., and McKean, M. E., A limited closure relation for anisotropic plasmas from the Earth's magnetosheath, *Phys. of Plasmas*, *1*, 1676, 1994.

Hill, P., Paschmann, G., Treumann, R. A., Baumjohann, W., and Sckopke, N., Plasma and magnetic field behavior across the magnetosheath near local noon, *J. Geophys. Res.*, *100*, 9575-9583, 1995.

Lees, L., Interaction between the solar plasma wind and the geomagnetic cavity, *AIAA J.*, *2*, 1576-1582, 1964.

Luhmann, J. G., Zhang, T.-L., Petrinec, S. M., Russell, C. T., Gazis, P., and Barnes, A., Solar cycle 21 effects on the interplanetary magnetic field and related parameters at 0.7 and 1.0 AU, *J. Geophys. Res.*, *98*, 5559, 1993.

Midgley, J. E. and Davis, L. J., Calculation by a moment technique of the perturbation of the geomagnetic field by the solar wind, *J. Geophys. Res.*, *68*, 5111-5123, 1963.

Paschmann G., Baumjohann, W., Sckopke, N., and Phan, T.-D., Structure of the dayside magnetopause for low magnetic shear, *J. Geophys. Res.*, *98*, 13409, 1993.

Petrinec, S. M. and Russell, C. T., Hydrodynamic and MHD equations across the bow shock and along the surfaces of planetary obstacles, *Space Sci. Rev.*, *79*, 757-791, 1997.

Phan, T.-D., Paschmann, G., Baumjohann, W., and Sckopke, N., The magnetosheath region adjacent to the dayside magnetopause: AMPTE/IRM observations, *J. Geophys. Res.*, *99*, 121, 1994.

Song, P. and Russell, C. T., What do we really know about the magnetosheath, *Adv. Space Res.*, *20*, 747-765, 1997.

Song, P., Russell, C. T., and Thomsen, M. F., Slow mode transition in the frontside magnetosheath, *J. Geophys. Res.*, *97*, 8295-8305, 1992.

Sonnerup, B. U. Ö., The reconnecting magnetopause, in *Magnetospheric Physics*, ed. by B.M. McCormac, 23, D. Reidel, Norwell, Mass, 1974.

Southwood, D. J. and Kivelson, M. G., Magnetosheath flow near the subsolar magnetopause: Zwan-Wolf and Southwood-Kivelson theories reconciled, *Geophys. Res. Let.*, *22*, 3275-3278, 1995.

Spreiter, J. R. and Stahara, S. S., Gasdynamic and magnetohydrodynamic modelling of the magnetosheath: A tutorial, *Adv. Space. Sci.*, *14*, 5-19, 1994.

Spreiter, J. R., Summers, A. L., and Alksne, A. Y., Hydrodynamic flow around the magnetosphere, *Planet. Space. Sci.*, *14*, 223, 1966.

Wu, C. C., MHD flow past an obstacle: Large scale flow in the

magnetosheath, *Geophys. Res. Lett.*, *19*, 87, 1992.

Zhang, T. L., Luhmann, J. G., and Russell, C. T., The solar cycle dependence of the location and shape of the Venus bow shock, *J. Geophys. Res.*, *95*, 11961, 1990.

Zhang, T. L., Russell, C. T., Luhmann, J. G., Spreiter, J. R., and Stahara, S. S., On the spatial range of validity of the gas dynamic model in the magnetosheath of Venus, *Geophys. Res. Lett.*, *20*, 751, 1993.

Zwan, B. L. and Wolf, R. A., Depletion of the solar wind plasma near a planetary boundary, *J. Geophys. Res.*, *81*, 1636–1648, 1976.